

# HAPCO: REAL TIME SIMULATION OF INTERACTION BETWEEN DEFORMABLE OBJECTS WITH HAPTIC FEEDBACK FOR SOLVING FRICTION MULTIPLE CONTACTS

Nadjet Talbi, Pierre Joli

*Laboratory IBISC, Evry Val d'Essonne university, 40 rue de Pelvoux, 91020 Evry, France*

Zhi-Qiang Feng

*Laboratory LME, Evry Val d'Essonne University, 40 Rue de Pelvoux, 91020 Evry, France*

Abderrahmane Kheddar

*Laboratory JRL, AIST Tsukuba Central 2, Umezono 1-1-1, Tsukuba 305-8568, Japan*

**Keywords:** Friction Contact, Interactive Simulation, Haptic rendering, Uzawa technic, Bi-potential Method.

**Abstract:** This paper deals principally with the comparison of two efficient algorithms to solve multi-contact problems with friction between two deformable bodies. These two algorithms are based on the bi-potential formulation of the contact laws, offering the control of the solution at each contact point through an unique mathematical operator of projection as well as a better force feedback stability of the friction contact force. For reasons of modular programming, a method to decouple the contact solver from the displacement solver is presented. A Haptic Contact simulator called "HapCo" has been developed as a prototype to test contact algorithms between two deformable objects in the context of interactive simulation with a haptic device.

## 1 INTRODUCTION

During the last twenty years, technologies related to medical areas have enormously improved; one of them is medical interactive simulators. The interest of interactive simulators based on advanced virtual and augmented reality techniques comes mainly from the surgeon's needs in terms of advanced teaching and training tools. Virtual Reality has been developed for many years in this context to reduce learning problems. The interactive simulation associated with multimodal rendering (haptic, visual, touch ...) provides medical operators the possibility to learn faster and easier. Surgical simulators are currently being developed at many research centers and companies (Gibson et al., 1997), (Cotin et al., 2000), (Zhuang, 2000) to create environments to help train physicians in the use of new surgical instruments and techniques in minimally invasive surgery. In this type of application, the numerical

context is soft body simulation based on physical models. Because surgical instruments are typically long slender structures, the contact points are limited to one point (point-based rendering) or some points along a segment (ray-based rendering) but never on a surface (surface-based rendering). However it could be interesting to consider for example the shape of a new surgical tool to test its efficiency in surgical tasks such as pulling, clamping, gripping and cutting soft tissue. Multiple contact points could be considered in that case between a rigid body (the tool) and the deformable object (the tissue). But in all complex simulated surgical tasks, we have to consider the organ-organ interaction through a surfaced distribution of contact points between two deformable bodies. In such a medical context of simulation, there is an ongoing quest for faster algorithms to solve multiple contact forces while controlling the numerical stability of the solution.

A real time simulation relies on three optimized

numerical “black boxes”, the first one to detect the potential contact points (collision detector), the second one to solve the nodal displacements of the discrete objects (displacement solver) and the third one to solve the multiple friction contact forces (contact solver). This paper concerns only descriptions about the contact solver. Interested readers may refer to (Teschner et al., 2004), (Lin, 1998) for a review of collision detectors and to (Erleben et al., 2005), (Gibson, 1997) about physics-based displacement solvers.

In the next section, we present a Haptic Contact simulator called “HapCo” developed in our laboratory as a prototype to test contact algorithms between two deformable objects in the context of interactive simulation with a haptic device. The important concept of the flexibility method is presented in which there is a separation between the computation of the contact forces and the computation of the nodal displacements.

The third section presents the formulation and the resolution of friction contact problems and it is focus on two efficient algorithms for the contact solver, called respectively “local Uzawa” and “global Uzawa”. They are both based on a bipotential formulation introduced by De Saxcé and Feng (De Saxce, 1991), (Feng, 1995). This formulation has the advantage to control the solution of the friction contact force. Finally we report and discuss the experimental results followed by some perspectives of future works.

## 2 DESCRIPTION OF THE “HAPCO” SIMULATOR

The Haptic Contact “HapCo” simulator is a prototype developed in our laboratory to test contact algorithms between two deformable bodies in the context of interactive simulation with a haptic device. These two bodies are parallelepiped (see figure 5), The red one can be clamped at its extremities and the green one can be manipulated in translation by the operator through a PHANTOM Desktop haptic interface (Sensable).

In the HapCo simulator, we use a linear elastic modelling of the bodies based on the Finite Element Method (FEM). We consider only quasi-static analysis because of very small inertial forces in medical applications. The linear elastic modeling is not really justified because it is only accurate for small deformations which is not the case of soft tissues (hyperelastic deformations). We have chosen

the linear modeling only for reasons of simplicity and computational efficiency. It is important to announce that our friction contact solver is suitable either for the non linear modeling or any other deformation modeling since it is based on the principle of flexibility (Francavilla, 1975) which allows to decouple the numerical task of the displacement solver from the numerical task of the friction contact force solver.

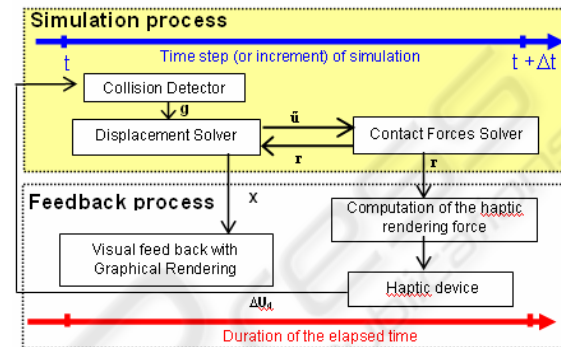


Figure 1: Data flow chart of the HapCo simulator.

The figure 1 describes the functional diagram of the interactive simulation in “HapCo”. When a collision is detected between the green body and the red one (see figure 5), the displacement solver computes the relative free displacement between the potential pairs of contact points. Then the contact solver gives the local contact forces  $r$  in order to avoid any interpenetration (Signorini condition) and to satisfy Coulomb laws (stick/slip phenomena).

Finally the displacement solver computes all the nodal positions of the two bodies by considering the contact forces as external (or given forces). The haptic rendering force is then computed from the given contact forces and sent back to the operator.

So this feedback force takes into account the stiffness of the two bodies and the friction contact laws (Signorini and Coulomb) of all contact points distributed on the contact surface. The next step of the simulation process is reinitialised from the new increment of rigid displacement given by the operator through the haptic device. The sample frequency of the elapsed time must be superior to 25 Hz to have an accurate visual rendering and superior to 300 Hz to have an accurate haptic force rendering (view). The main objective of HapCo is to test different algorithms to solve multi friction contact problem in order to determinate which one gives the best stable force feedback in real-time.

### 3 ALGORITHMIC PRINCIPLE

We propose to follow an incremental mixed formulation (displacement and contact force) of the equilibrium equations and to solve separately the contact force by successive local projections of these equations in the local reference frames at contact points. This method is called the flexibility method because it consists of establishing a flexibility matrix (Francavilla, 1975) or a Delassus operator (Duriez, 2005).

In order to calculate the friction contact forces, the contact laws (Signorini and Coulomb) are formulated from an augmented Lagrangian formulation (bi-potential formulation) and computed by an Uzawa technique which leads to an iterative predictor/corrector process. The bipotential method proposed by De Saxcé and Feng (Feng, 2003), (Feng, 1995) provides a powerful tool to model dissipative constitutive laws such as Coulomb friction laws. The figure 2 describes the basic principle of this method. Interested readers can find more details in (De Saxcé, 1991 and Wriggers, 2002).

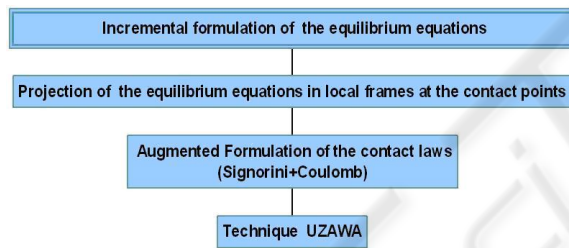


Figure 2: Principle Algorithm.

#### 3.1 Incremental Formulation of Equilibrium Equations

The following equation governs the quasi static nonlinear problems involving contact between finite element bodies:

$$\mathbf{F}_{\text{int}} + \mathbf{F}_{\text{ext}} + \mathbf{R} = \mathbf{0}$$

where  $\mathbf{F}_{\text{int}}$  is the vector of internal nodal forces,  $\mathbf{F}_{\text{ext}}$  denotes the vector of external nodal forces and  $\mathbf{R}$ , the vector of nodal contact forces.

This equation is strongly nonlinear with respect to the nodal displacements  $\mathbf{U}$ , because of finite strains and large displacements. The incremental formulation consists of writing a linear relation of the internal forces relative to  $\mathbf{U}$ . A Newton-Raphson iterative resolution is carried out as follows:

$$\begin{cases} \mathbf{K}_T^i \Delta \mathbf{U} = \mathbf{F}_{\text{int}}^i + \mathbf{F}_{\text{ext}} + \mathbf{R}^i \\ \mathbf{U}^{i+1} = \mathbf{U}^i + \Delta \mathbf{U} \end{cases}$$

where  $i$  is the iteration number at which the equations are computed.  $\mathbf{K}_T^i$  is the tangent stiffness matrix and  $\Delta \mathbf{U}$  is the correction vector of the nodal displacements. Taking the derivative of  $\mathbf{F}_{\text{int}}$  with respect to  $\mathbf{U}$  gives the tangent stiffness matrix:

$$\mathbf{K}_T = -\frac{\partial \mathbf{F}_{\text{int}}}{\partial \mathbf{U}}$$

It is noted that the incremental formulation of the equilibrium equations can not be solved directly since  $\Delta \mathbf{U}$  and  $\mathbf{R}$  are both unknown. The key idea is to determine first  $\mathbf{R}$  in a reduced system which only concerns the contact nodes. Then  $\Delta \mathbf{U}$  can be computed in the whole structure, using contact reactions as external forces. In the following section, we describe how to determine the contact forces.

#### 3.2 Friction Contact Formulation

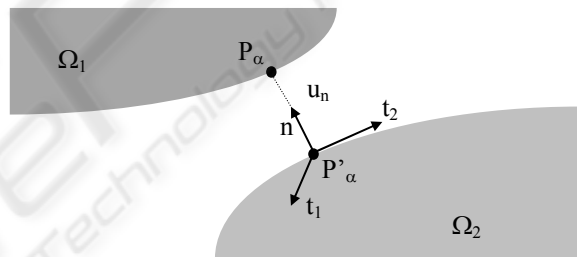


Figure 3: Local coordinate frame at the contact point  $\alpha$ .

The unilateral contact law in the case of deformable objects is characterized by a linear relationship between the constraint displacement  ${}^\alpha \mathbf{u}$  and the contact force  ${}^\alpha \mathbf{r}$ , for each pair of contact points  $\alpha = (1..m)$  as shown in figure 3. This relation can be written as:

$$\mathbf{W}_{\alpha\alpha} {}^\alpha \mathbf{r} + {}^{\alpha\beta} \mathbf{u} + {}^\alpha \tilde{\mathbf{u}} = {}^\alpha \mathbf{u}$$

where  $\mathbf{W}_{\alpha\alpha}$  and  ${}^\alpha \tilde{\mathbf{u}}$  represent respectively the local flexibility matrix (3x3dimension) and the free displacement at the contact point  $\alpha$  (i.e. when all the contact forces are zero).  ${}^{\alpha\beta} \mathbf{u}$  is the displacement at the contact point  $\alpha$  induced by the contact forces occurring at contact points  $\alpha \neq \beta$ .  ${}^\alpha \mathbf{u}$ ,  ${}^{\alpha\beta} \mathbf{u}$  and  ${}^\alpha \mathbf{r}$  are defined relative to the local coordinate frame positioned at the contact point  $\alpha$ . The flexibility matrix depends on the local stiffness of each object in contact and the free displacement depends on the internal forces and the external forces applied to

each object in contact.

This equation represents a system of 3 scalar equations where the local unknowns are  ${}^\alpha \mathbf{u}$  and  ${}^\alpha \mathbf{r}$  (6 scalar unknowns). To describe the local behavior of each contact point  $\alpha$  additive constraints are necessary.

The unilateral contact law is characterized by a geometric condition of non-penetration, a static condition of no-adhesion and a mechanical complementary condition. These three conditions are known as Signorini conditions expressed, for each contact point  $\alpha$ , in terms of the normal signed constrained displacement  ${}^\alpha \mathbf{u}_n = {}^\alpha \mathbf{u} \cdot \mathbf{n}$  and the normal signed contact force  ${}^\alpha r_n = {}^\alpha \mathbf{r} \cdot \mathbf{n}$  by:

$$\text{Signor}({}^\alpha u_n, {}^\alpha r_n) \Leftrightarrow {}^\alpha u_n \geq 0, {}^\alpha r_n \geq 0 \text{ and } ({}^\alpha u_n) {}^\alpha r_n = 0$$

The classical Coulomb friction rule is defined by:

$$\text{Coul}({}^\alpha \mathbf{u}_t, {}^\alpha \mathbf{r}_t) \Leftrightarrow \text{If } \|\alpha \mathbf{u}_t\| = 0 \text{ then } \|\alpha \mathbf{r}_t\| \leq \mu {}^\alpha r_n$$

$$\text{else } \alpha \mathbf{r}_t = -\mu \frac{\alpha \mathbf{u}_t}{\|\alpha \mathbf{u}_t\|}$$

Where  $\mu$  is the coefficient of friction and  ${}^\alpha \mathbf{u}_t$  (resp.  ${}^\alpha \mathbf{r}_t$ ) is the tangential part of  ${}^\alpha \mathbf{u}$  (resp.  ${}^\alpha \mathbf{r}$ ).

The complete contact laws (Signorini condition + Coulomb friction laws) can be defined by the three contact states as follows:

- ${}^\alpha u_n > 0$  and  ${}^\alpha r_n = 0$  (Separating)
- $\begin{cases} \|\alpha \mathbf{u}_t\| = 0 \\ \text{and } \alpha \mathbf{r}_t \in \text{int}(K_\mu^\alpha) \end{cases}$  (Contact with sticking)
- $\begin{cases} \|\alpha \mathbf{u}_t\| \neq 0 \\ \text{and } \alpha \mathbf{r}_t \in \text{bd}(K_\mu^\alpha) \\ \text{with } \alpha \mathbf{r}_t = -\mu \frac{\alpha \mathbf{u}_t}{\|\alpha \mathbf{u}_t\|} \end{cases}$  (Contact with sliding)

Where  $K_\mu^\alpha$  is the so-called Coulomb cone at the contact point  $\alpha$  and represents the set of admissible forces defined by:

$$K_\mu^\alpha = \left\{ \mathbf{r}^\alpha \in R^3 \text{ tel que } {}^\alpha r_n \geq 0 \text{ et } \|\alpha \mathbf{r}_t\| - \mu {}^\alpha r_n \leq 0 \right\}$$

The terms  $\text{int}(K_\mu^\alpha)$  and  $\text{bd}(K_\mu^\alpha)$  are respectively the interior and the surface of the Coulomb cone. The contact laws give no explicit relation between  ${}^\alpha \mathbf{r}_t$  and  ${}^\alpha \mathbf{u}_t$  in case of contact with sticking and in case of no contact.

Based on the augmented lagrangian method

used to solve contact problems (Alart, 1991 and Simo, 1992), De Saxcé and Feng have proposed to use the bi-potential formulation to write the complete contact laws by the following projection operator:

$${}^\alpha \mathbf{r} = \text{Proj}_{K_\mu}({}^\alpha \mathbf{r}^*)$$

$$\text{with } \begin{cases} \alpha \mathbf{r}^* = \alpha \mathbf{r} - \rho \alpha \mathbf{u}^* \\ \alpha \mathbf{u}^* = \alpha \mathbf{u} + \mu \|\alpha \mathbf{u}_t\| \mathbf{n} \end{cases}$$

Where  ${}^\alpha \mathbf{r}^*$  is the so-called augmented contact force at the contact point  $\alpha$ .  $\text{Proj}_{K_\mu}$  is the projection operator on the Coulomb cone.  $\rho$  is an arbitrary positive parameter. The three possible contact states are illustrated in figure 4.

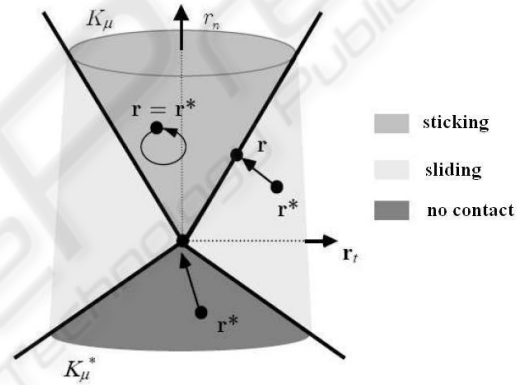


Figure 4: Coulomb cone projection and contact states.

Within the bi-potential framework, the projection operation can be explicitly defined by:

$$\text{Proj}_{K_\mu}({}^\alpha \mathbf{r}^*) = \alpha \mathbf{r}^* \text{ si } \|\alpha \mathbf{r}_t^*\| \leq \mu r_n^* \text{ Sticking}$$

$$\text{Proj}_{K_\mu}({}^\alpha \mathbf{r}^*) = 0 \text{ si } \mu \|\alpha \mathbf{r}_t^*\| \leq -r_n^* \text{ No Contact}$$

$$\text{Proj}_{K_\mu}({}^\alpha \mathbf{r}^*) = \alpha \mathbf{r}^* - \left( \frac{\|\alpha \mathbf{r}_t^*\| - \mu r_n^*}{1 + \mu^2} \right) \left( \frac{\alpha \mathbf{r}_t^*}{\|\alpha \mathbf{r}_t^*\|} - \mu \mathbf{n} \right) \text{ Sliding}$$

### 3.3 Friction Contact Resolution

From the above equations and by considering  $m$  contact points, we have to solve successively  $m$  local systems ( $\alpha=1, m$ ) described as:

$$\begin{cases} \alpha \mathbf{u} - \mathbf{W}_{\alpha\alpha} \alpha \mathbf{r} - \alpha \beta \mathbf{u} - \alpha \tilde{\mathbf{u}} = 0 \\ \alpha \mathbf{r} - \text{Proj}_{K_\mu}({}^\alpha \mathbf{r}^*) = 0 \end{cases}$$

These  $m$  local systems are implicitly dependent

because of  ${}^{\alpha\beta}\mathbf{u}$  which has the following expression:

$${}^{\alpha\beta}\mathbf{u} = \sum_{\substack{\beta=1,m \\ \alpha \neq \beta}} \mathbf{W}_{\alpha\beta} {}^{\beta}\mathbf{r}$$

Where each  $\mathbf{W}_{\alpha\beta}$  can be considered as an influence matrix between two contact points  $\alpha$  and  $\beta$ . To solve these local systems, we propose the two following approaches:

### 3.3.1 Local Uzawa Approach

The non linear iterative Gauss Seidel algorithm consists of solving successively the  $m$  local systems at each iteration  $k$ :

$$\begin{cases} \alpha \mathbf{u}^{(k+1)} - \mathbf{W}_{\alpha\alpha} \alpha \mathbf{r}^{(k+1)} - \alpha\beta \mathbf{r}^{(k+1)} \mathbf{u} - \alpha \tilde{\mathbf{u}} = 0 \\ \alpha \mathbf{r}^{(k+1)} - \text{Proj}_{K_{\mu}} (\alpha \mathbf{r}^{(k+1)*}) = 0 \end{cases}$$

$${}^{\alpha\beta}\mathbf{u}^{(k+1)} = \sum_{\beta=1,\alpha-1} \mathbf{W}_{\alpha\beta} {}^{\beta}\mathbf{r}^{(k+1)} + \sum_{\beta=\alpha+1,m} \mathbf{W}_{\alpha\beta} {}^{\beta}\mathbf{r}^{(k)}$$

Until we obtain the numerical convergence defined by:

$$\|\mathbf{r}^{(k+1)} - \mathbf{r}^{(k)}\| < \varepsilon_1 \quad \mathbf{r}^{(k)} = (r^{(k)}, \dots, r^{(k)})$$

where  $\varepsilon_1$  is the numerical tolerance of the global contact force which can be related to the precision of the haptic device. The initial value is  $\mathbf{r}^{(0)} = 0$ .

Now we have to solve for each local system the unknowns  ${}^{\alpha}\mathbf{u}^{(k+1)}$  and  ${}^{\alpha}\mathbf{r}^{(k+1)}$ . The numerical solution can be carried out by means of the Uzawa algorithm which leads thus to an iterative process:

$$\begin{aligned} \alpha \mathbf{r}^{*(k+1)(j+1)} &= \alpha \mathbf{r}^{(k+1)(j)} - \rho (\alpha \mathbf{u}^{(k+1)(j)} + \mu \|\alpha \mathbf{u}_t^{(k+1)(j)}\| \mathbf{n}) \\ \alpha \mathbf{r}^{(k+1)(j+1)} &= \text{Proj}_{K_{\mu}} (\alpha \mathbf{r}^{*(k+1)(j+1)}) \\ \alpha \mathbf{u}^{(k+1)(j+1)} &= \mathbf{W}_{\alpha\alpha} \alpha \mathbf{r}^{(k+1)(j+1)} + \alpha\beta \mathbf{u}^{(k+1)} + \alpha \tilde{\mathbf{u}} \end{aligned}$$

The numerical convergence is given by:

$$\frac{\|\alpha \mathbf{r}^{(k+1)(j+1)} - \alpha \mathbf{r}^{(k+1)(j)}\|}{\rho} < \varepsilon_2$$

$\varepsilon_2$  is a second numerical tolerance which can be related to the desired visual rendering or to the physical interpenetration tolerance which can be estimated from characteristic lengths of the objects in contact. The initial values are  ${}^{\alpha}\mathbf{r}^{(k+1)(0)} = 0$  and  ${}^{\alpha}\mathbf{u}^{(k+1)(0)} = \alpha\beta \mathbf{u}^{(k+1)} + \alpha \tilde{\mathbf{u}}$ .

We call this approach the ‘‘local Uzawa’’. Indeed, the two presented iterative processes compute all the contact forces with two levels of

control. One is local to each contact point and based on visual rendering and the other is global and based on the haptic rendering.

### 3.3.2 Global Uzawa Approach

Another way is to have a control only on the haptic rendering by considering only one predictor corrector step in the Uzawa algorithm:

- Predictor step:  
 $\alpha \mathbf{r}^{*(k+1)} = \alpha \mathbf{r}^{(k+1)} - \rho (\alpha \mathbf{u}^{(k)} + \mu \|\alpha \mathbf{u}_t^{(k)}\| \mathbf{n})$
- Corrector step  
 $\alpha \mathbf{r}^{(k+1)} = \text{Proj}_{K_{\mu}} (\alpha \mathbf{r}^{*(k+1)})$
- Back up the new constrained displacement  
 $\alpha \mathbf{u}^{(k+1)} = \mathbf{W}_{\alpha\alpha} \alpha \mathbf{r}^{(k+1)} + \alpha\beta \mathbf{u}^{(k+1)} + \alpha \tilde{\mathbf{u}}$

We call this approach the ‘‘global Uzawa’’. Many examples have been successfully treated (Feng, 1995 and 2003) with the global Uzawa approach but only in a standard simulation process (non interactive). In these examples the numerical convergence is given by:

$$\frac{\|\mathbf{r}^{(k+1)} - \mathbf{r}^{(k)}\|}{\mathbf{r}^{(k+1)}} < \varepsilon_3$$

In computational mechanics,  $\varepsilon_3$  is just a very small parameter (relative error) related only to a desire of a high numerical precision.

### 3.3.3 Comparison and Results

To compare the local and global Uzawa approaches, we consider the following benchmark:

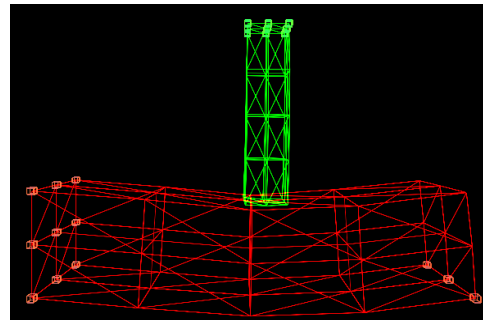
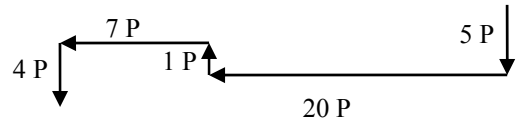


Figure 5: Numerical benchmark 1.

The highlighted points on the upper surface of

the green object move along 5 series of rigid displacements as described in figure 5. Every unit displacement  $P$  is equal to 0.1cm. The red object is clamped on its extremities at the highlighted nodal points (see figure 6). The green object and the red one have respectively 80 000 and 3000 as Young modulus. Both objects have the same Poisson ratio equal to 0,3. The dimensions of the clamped elastic solid are  $L=10, W=2, H=2$  (cm). Initially, the two objects are not deformed and are in contact (no interpenetration). The computer used is a Pentium 4 with 1.75 Ghz and 1.5 Go of RAM.

Simulation results are shown in figures 7 and 8. In the second numerical benchmark, the red object is fixed from only the left extremity. That makes this benchmark less stiff than the previous one, numerical results are shown in figure 9. For both algorithms (local and global Uzawa), we choose to control only the physical interpenetration tolerance, then all the numerical convergence thresholds  $\varepsilon_1, \varepsilon_2$  and  $\varepsilon_3$  are defined by:

$$\frac{\|\alpha_{\mathbf{r}}^{(k+1)} - \alpha_{\mathbf{r}}^{(k)}\|}{\rho} < \text{Uzawa Error} \quad \rho = \text{Min} \left( \frac{1}{W_{ii}} \right) \quad i = 0, 3m$$

$\rho$  is equivalent to a stiffness and must be inferior to the smallest local stiffness at the contact points.

The figures 6, 7, and 8 are divided in 5 phases according to the 5 rigid displacements series. We note that the iteration numbers  $k$  in the local Uzawa resolution are lower than the iteration numbers  $k$  obtained for the Gauss-Seidel resolution in the five simulation phases.

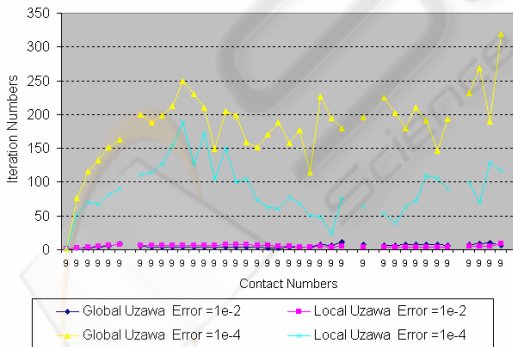


Figure 6: Friction coefficient = 0.3.

This result has been observed several times (as shown in figure 7), for different values of the friction coefficient (from 0.0 to 0.6) and for different values of the Uzawa error. We observe from the graph 8 that the Uzawa error has an important role on the convergence time for the two resolution

techniques. Indeed, if the resolution precision increases, then, the CPU time increases as well. This result has been observed with many friction coefficients. We can also note that local Uzawa solver has a tendency to be faster than the global Uzawa one. Figure 9 points out instabilities with the global Uzawa solver.

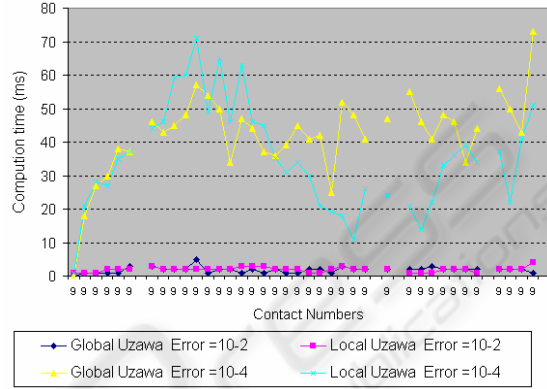


Figure 7: Friction coefficient = 0.3.

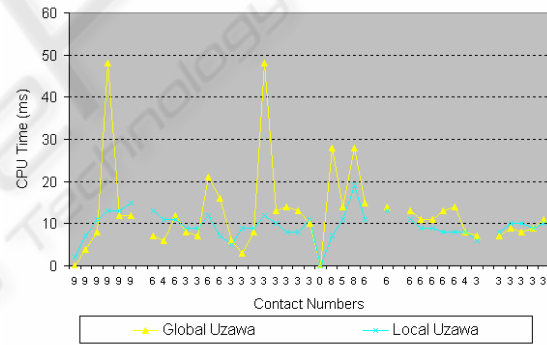


Figure 8: Friction coefficient= 0.6, Uzawa Error =1e-4.

## 4 CONCLUSIONS

The HapCo simulator represents our first contribution to bridge two domains, the computational mechanics and the haptic rendering in the context of Virtual Reality. This real time simulator with haptic feedback force includes elastic deformable objects, collision detection between interacting bodies, friction contact force computation and displacement solver based on the Finite Element Method.

We have successfully tested the local and global Uzawa algorithm described above with the bi-potential approach. The results obtained seem to indicate that the local Uzawa solver is faster and

more stable than the global Uzawa solver.

By changing the friction coefficient we can feel the slip/stick contact force. Many people have tested the HapCo simulator and have been surprised by the quality of the haptic rendering.

We need more numerical tests to conclude about the computational efficiency of the two algorithms. Indeed, if the application works very well when the moving object comes into contact with the very soft parts of the clamped object, we find some numerical instabilities when the contact occurs with the stiff parts (near the fixed nodal points). These difficulties have two origins. The first one is when the operator does not handle firmly the haptic device and can be surprised by the increase in rigidity while he is moving towards rigid part. The second one is due to excessive free displacement  $\tilde{u}$  when the contact occurs. The greater this quantity is, the greater the number of iterations is and so the real time constraint is no longer satisfied. To overcome this difficulty, the operator has to move gently when he comes into contact with the stiff parts. To help the operator we suggest zooming around the contact area in order to augment the control of his gesture by a better visual feedback.

We are working to optimize and to accelerate the simulation algorithm by considering closer the sparseness of the matrices and vector manipulated during the process. This is in order to consider non linear elasticity modeling and large multi-contact problems: childbirth simulation for example.

## REFERENCES

- De Saxcé, G., Feng Z.Q., 1998. "The bipotential method: a constructive approach to design the complete contact law with friction and improved numerical algorithms". *Mathematical and Computer Modeling, special issue, « Recent Advances in Contact Mechanics », 28(4-8), 225-245.*
- Alart, P., Curnier, A., 1991. "A mixed formulation for frictional contact problems prone to Newton like solution methods". *Comp. Meth. Appl. Mech. Engng., 92, 353-375.*
- Simo, J.C., Laursen, T.A., 1992. "An augmented Lagrangian treatment of contact problems involving friction". *Computers & Structures, 42, 97-116.*
- De Saxcé, G., Feng, Z.Q., 1991. "New inequality and functional for contact with friction": The implicit standard material approach. *Mech. Struct. & Mach., 19, 301-325.*
- Feng, Z.Q., 1995. "2D or 3D frictional contact algorithms and applications in a large deformation context". *Comm. Numer. Meth. Engng., 11, 409-416.*
- Feng, Z.Q., Peyraut, F., Laped, N., 2003. "Solution of large deformation contact problems with friction between Blatz-Ko hyperelastic bodies". *Int. J. Engng. Science, 41, 2213-2225.*
- Duriez, C., Dubois, F., Kheddar, A., Andriot, C., 2005. "Realistic haptic rendering of interacting deformable objects in virtual". *IEEE trans. on visualization and computer Graphics.*
- Wriggers, P., 2002. "Computational contact mechanics". *John Wiley & Sons.*
- Gibson, S.F.F., Mirtich, B., 1997. "A survey of deformable modeling in computer graphics". *Tech. Report No. TR-97-19, Mitsubishi Electric Research Lab, Cambridge, MA.*
- Cotin, S., Delingette, H., Ayache, N., 2000. "A hybrid elastic model allowing real-time cutting, deformations, and force feedback for surgery training and simulation". *Visual Computer, vol. 16, no. 7, pp. 437-452.*
- Basdogan, G., De, S., Kim, J., Muniyandi, M., Kim, H., Srinivasan, M.A., 2004. "Haptics in minimally invasive surgical simulation and training". *IEE Computer Society, Haptic Rendering-Beyond Visual Computing, pp 56-64.*
- Zhuang, Y., Canny, J., 2000. "Haptic interaction with global deformations". *IEEE ICRA, San Francisco, (pp20, 21, 88).*
- Francavilla, A., Zienkiewicz, O.C., 1975. "A note on numerical computation of elastic contact problems". *Int. Num. Meth. Eng. 9, 913-924.*
- Teschner, M., Kimmerle, S., Heidelberg, B., Zachmann, G., Raghupathi, L., Fuhrmann, A., Cani, P., Faure, F., Magnenat-Thalmann, N., Strasser, W., Volino P., 2004. Detection for deformable objects. Eurographics, STAR (State of The Art Report), pp. 119-135..
- Lin, M. C., Gottschalk, S., 1998. Collision Detection between Geometric Models: A survey. Proc. of IMA Conference on Mathematics of surfaces, pp. 37-56.
- Erleben, K., Sporring, J., Henriksen, K., and Dohlmann, H., 2005. Physics-Based Animation, Charles River Media, Inc..
- Gibson, S. F., Mirtich, B., 1997, A survey of deformable modeling in computer graphics. Tech. Report No. TR-97-19, Mitsubishi Electric Research Lab, Cambridge, MA.